Title
New RSL constraints for the Minch from OSL-dated Lateglacial shorelines

Journal
Quaternary Science Reviews, 367

ISSN
0277-3791

Authors
Huffman, Emily
Simms, Alexander R
Bradwell, Tom
et al.

Publication Date
2025-11-01

DOI
10.1016/j.quascirev.2025.109543

New RSL constraints for the Minch from OSL-dated Lateglacial shorelines

Emily Huffman[1], Alexander R. Simms[1], Tom Bradwell[2], Louise Best[3],
Jeremy M. Lloyd[4], Sarah L. Bradley[5], Regina DeWitt [6]

[1] Department of Earth Science, University of California, Santa Barbara, CA, USA
[2] Faculty of Natural Sciences, University of Stirling, Scotland, UK
[3] School of Education and Science, University of Gloucestershire, Cheltenham, UK
[4] Department of Geography, Durham University, Durham, UK
[5] School of Geography and Planning, University of Sheffield, Sheffield, UK
[6] Department of Physics, East Carolina University, Greenville, NC, USA

Abstract

Past sea levels provide important constraints on global ice volumes, rates of tectonic motion, ice-sheet sea-level feedbacks, and the migration of species through time. Beneath formerly glaciated regions, the marine limit, the maximum extent of sea-levels after glacial retreat, provides some of the oldest post-Last Glacial Maximum (LGM) sea-level constraints. However, although the elevations of marine limits are plentiful, they often remain undated. In this study, we provide new age and elevation constraints on the late Pleistocene relative sea-level (RSL) history at 12 sites along the eastern flanks of the former Minch Ice Stream (MnIS) of northwest Scotland. Optically stimulated luminescence (OSL) was used to date the highest and presumably oldest preserved RSL indicators immediately after ice-sheet retreat. Although slightly older than earlier estimates, our ages confirm the early deglacial age of ~16.2-19.5 ka for the raised shorelines of northwest Scotland with declining marine limits north of the Isle of Skye from 26.2 ± 4.8 m at Ardaneaskan to 12.8 ± 4.8 m elevation at Achiltibuie, the latter of which lies inside the moraines of the Wester Ross Readvance. Our new OSL ages suggest deglaciation of the MnIS may have been slightly earlier than previously thought, although our large error bars highlight the need for additional age constraints. Our new RSL data provide important constraints for Glacial Isostatic Adjustment (GIA) models for Scotland and shed light on the behavior of the former MnIS, thought to be susceptible to marine ice-sheet instability.

1. Introduction

Understanding the interactions between ice sheets and sea-level change is critical for predicting the future response of ice sheets to climate change and rising global sea levels. One of the largest unknowns is the future response of large, fast-flowing marine-terminating glaciers or ice streams, which may be susceptible to marine-ice sheet instability (MISI) (IPCC, 2019; Schoof, 2007). MISI is characterized by the collapse of ice sheet sectors extending seaward over a landward sloping bed. If modern day ice sheets are susceptible to MISI, they would accelerate rates of future sea-level rise “(Gornitz et al. 2019; Bamber et al. 2019; Ritz et al. 2015; DeConto et al. 2016; Pattyn et al. 2018). However, sea-level feedbacks (SLFs) may counteract MISI by stabilizing ice sheets through retreat-induced uplift of the seafloor (Gomez et al. 2010; Schoof, 2007).

One way to better understand these SLFs is to examine the past behavior of ice streams. One such paleo ice stream that may have undergone MISI is the Minch Ice Stream (MnIS) of NW Scotland (Gandy et al. 2018; Bradley et al. 2011). RSL can provide a glimpse into the role GIA-driven RSL changes may have played in the retreat of this ice stream (Simms et al. 2022). However, despite over a century of work documenting past RSL changes across Scotland, gaps in the RSL data required to constrain GIA models for the region remain (Shennan et al. 2018; Bradley et al. 2011; Smith et al. 2019; Horton et al. 2020). One particularly poorly constrained component of the RSL record for mainland NW Scotland, around the former MnIS, is the age of the marine limit, which in this location is marked by a raised shoreline known locally as the “Lateglacial shoreline”.

Traditionally, one of the difficulties in constraining the age of the Lateglacial shoreline is the absence of radiocarbon datable material. However, with the abundance of quartz and feldspars within Lateglacial shoreline deposits, optically stimulated luminescence (OSL) dating provides a potentially fruitful avenue for dating these shorelines. OSL determines the time elapsed since minerals were last exposed to sunlight, specifically their burial age (Huntley et al. 1985; Rhodes, 2011; Murray et al. 2021). The quartz-rich Torridonian Sandstone and Lewisian

Gneiss bedrock of much of NW Scotland offers suitable materials for the production of quartz sand.

This study aims to determine the age of the Lateglacial and other post-glacial shorelines across the eastern Minch (in NW Scotland) using OSL. These ages, along with their elevations, will provide new RSL constraints for NW Scotland following deglaciation. These new constraints also provide important data for determining what role, if any, RSL may have played in the retreat history of the MnIS.

2. Background

2.1 Ice Reconstruction: Brief History of the British and Irish Ice Sheets (BIIS and FIS) and the Minch Ice Stream (MnIS)

During the LGM, the British-Irish Ice Sheet (BIIS) covered most of the British Isles and extended onto the adjacent continental shelf, merging to the east with the Fennoscandian Ice Sheet (FIS) at the peak of the LGM and forming a vast ice mass covering much of northern Europe (Bradwell et al. 2008, 2021; Hughes et al. 2016; Ballantyne and Small 2019). At this time, its margins were drained by several ice streams including the MnIS, the ice stream that filled the 40-50 km wide channel between the Outer Hebrides and mainland NW Scotland (Fig. 1) (Bradwell and Stoker, 2015; Bradwell et al. 2019). The MnIS drained the northwest sector of the BIIS at various times over the last glacial cycle (Fig. 1) (Bradwell et al. 2008, 2019; Bradwell and Stoker, 2015; Ballantyne and Small, 2019).

At its height, the MnIS discharged approximately 12-20 Gt/a of ice (Bradwell and Stoker, 2015, Bradwell et al. 2019). The MnIS underwent a steady retreat from 30 to 18.5 ka followed by a collapse of its western branch between 18.5 and 16.9 ka, and a pronounced retreat of its eastern branch from 16.9 to 15.9 ka (Bradwell et al. 2019; 2021). Simms et al. (2022) confirmed the timing of rapid retreat of the eastern MnIS, approximately 17.6-16.4 ka, based on ^{14}C dating of isolation basin deposits along the eastern flanks of the former MnIS.

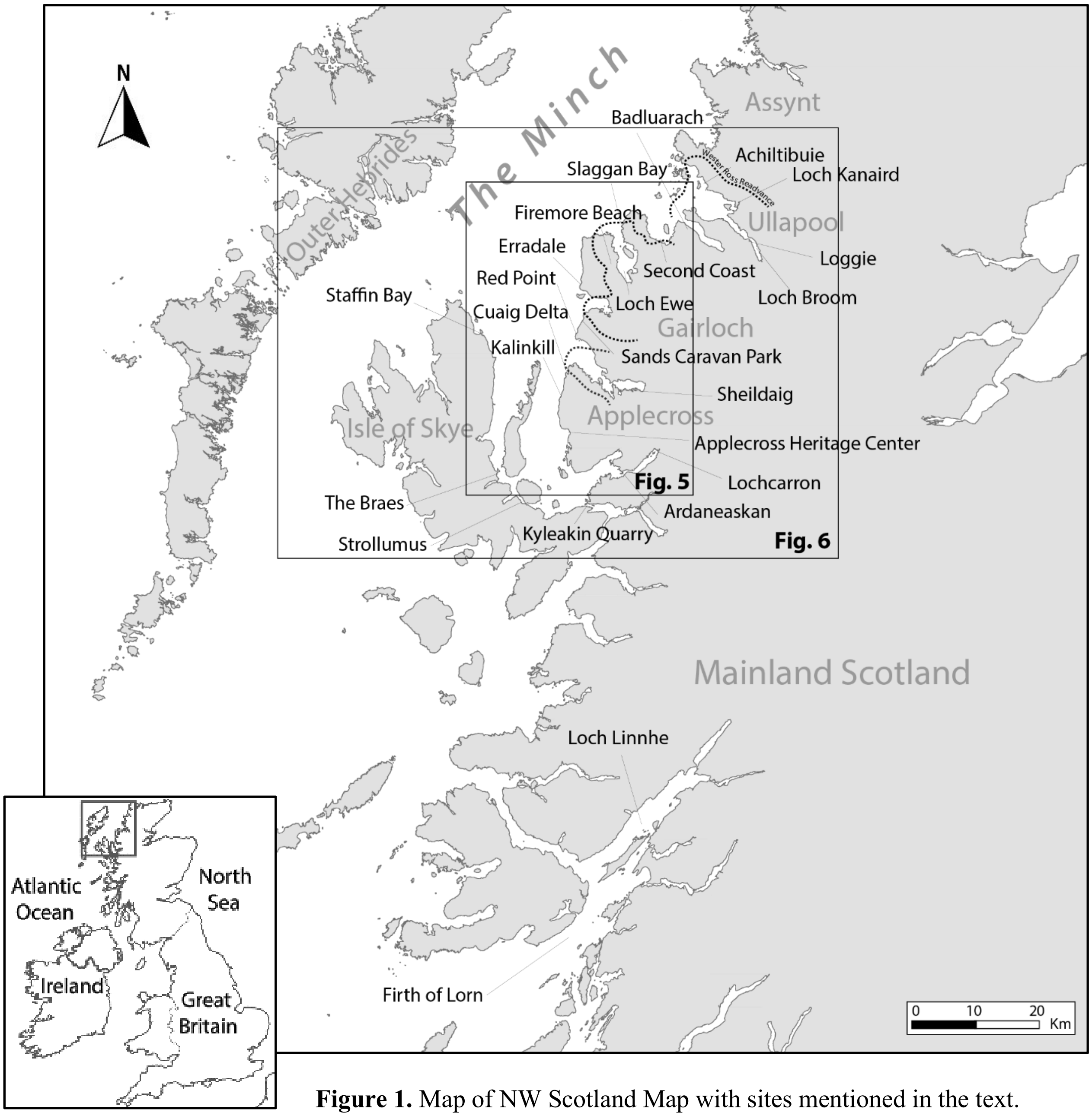

Figure 1. Map of NW Scotland Map with sites mentioned in the text.

2.2 Wester Ross Readvance

The Wester Ross Readvance (WRR) was a local readvance of glaciers identified in the Wester Ross area of NW Scotland (Fig. 1). Its moraines record a significant glacier oscillation after the LGM (26-22 ka) but prior to the Younger Dryas Stadial (12.9-11.7 ka) (Robinson and Ballantyne, 1979; Sissons and Dawson, 1981). Everest et al. (2006) were the first to date the WRR moraines with Terrestrial Cosmogenic Nuclide (TCN) dating, deriving a mean exposure age near Gairloch (Fig. 1) of 16.3 ± 1.6 ka from 3 boulders. Bradwell et al. (2008) obtained 8 more TCN ages from WRR moraines further north around Achiltibuie and Little Loch Broom (mean age = 13.5 ka); followed by Ballantyne et al (2009) who, in a wider study, reported similar ages from 5 other moraines across Wester Ross (14.0-13.5 ka). Ballantyne and Stone (2012) recalibrated these ages to show that the originally reported WRR ages (n=22) were probably too young. Ballantyne and Small (2019) recalibrated these ages a second time using an updated scaling scheme and revised production rate to yield a mean age (for all 22 TCN ages) of 15.3 ± 0.7 ka for the WRR moraine. Using Bayesian sequence modeling of the same (recalibrated) TCN ages, Bradwell et al. (2021) placed the WRR retreat between 14.6-15.6 ± 1.0 ka. More recently, Simms et al. (2022) constrained the age of WRR glacier retreat around Gairloch to 15.8 ± 0.1 ka, based on radiocarbon ages from isolation basins within the margins of the WRR. These differences in age assessment for the WRR have led to different interpretations including: a regional-scale glacier response to cooling associated with Heinrich Event 1 (H1) (Everest et al. 2006; Ballantyne and Stone, 2012; Bradwell et al. 2021); tidewater-driven glacier instability (Bradwell et al. 2021); or a dynamic drawdown of mainland ice due to the evacuation of ice in the Minch (Simms et al. 2022). The WRR is also important as the marine limit is generally *lower* inside its moraine limits than outside, confirming that at least one significant glacier fluctuation occurred along the western seaboard of mainland NW Scotland during ice-sheet deglaciation.

2.3 Post LGM Sea Level changes in NW Scotland

Following deglaciation around 14-16 ka, RSLs in NW Scotland were estimated to be approximately 30-35 m above present-day sea level (Best and Shennan, 2024; Best et al., 2022; Simms et al., 2022; Bradley et al., 2023; Smith et al., 2019; Shennan et al., 2018). From this marine limit at 14-16 ka, RSLs fell rapidly, reaching a lowstand below present-day sea level in many areas between 10-12 ka (Bradley et al., 2023; Hamilton et al., 2015; Smith et al., 2019; Shennan et al., 2018). Subsequently, RSLs rose to the mid-Holocene highstand with variable altitudes across the region, but reaching a maximum of 5-8 m above present from 6-8 ka before falling to present day levels (Selby and Smith, 2007; Hamilton et al. 2015; Smith et al. 2019; Shennan et al. 2018; Best et al. 2022; Bradley et al. 2023).

2.4 Lateglacial Shoreline

Raised coastal features of the Lateglacial shoreline in NW Scotland record the first ice-free conditions immediately after the LGM and represent the oldest preserved post-LGM RSL indicators. McCann (1966) mapped a single raised shoreline, now known as the Lateglacial shoreline but referred to then as the 25-foot raised beach (Wright, 1911), across western Scotland between the Firth of Lorn and Loch Broom (Fig. 1). Previous studies indicated that features associated with the 25-foot beach include shore and wave-cut platforms, marine terraces, storm-beach ridges, shingle and sand beaches, and deltas (Wright 1911, 1914). Despite being extensively mapped five decades ago (Robinson, 1977; Sisson and Dawson, 1981), these raised shorelines remain largely undated across much of NW Scotland. One of the few dated shoreline sequences are those of west Jura and northeast Islay, to the south of our study area (Fig. 1), with the oldest and highest shorelines dating to between ~15.7-16.3 ka based on TCN ages on raised beach cobbles (Dawson et al. 2022).

One primary factor contributing to the variable elevation of the Lateglacial shoreline is differential rebound of the Earth's crust following glacial retreat (Lin et al. 2021; Peltier, 1998; Shennan et al. 2018). Due to the spatial variations in thickness and distribution of ice across NW Scotland during the last glacial period, the main Lateglacial shoreline decreases in elevation in all westerly directions away from Loch Linnhe with an estimated overall tilting of the shoreline in a WNW direction (McCann, 1966) (Fig. 1). Similarly, Sissons et al. (1976) constructed a generalized isobase map for the Lateglacial shoreline indicating the shoreline declining to the northwest for NW Scotland. A follow-up study by Sissons and Dawson (1981) estimated the shoreline sloping down to the NNW between 0.33 and 0.39 m/km.

3. Methods

3.1 Surveying of the Raised Shorelines

Elevations of post-LGM shoreline features were surveyed at 16 locations across NW Scotland (Fig. 6, Table 1). Mapped raised marine features by Peach et al. (1910), Anderson and Dunham (1966), Walker et al. (1988), Ballantyne et al. (2010), Robinson (1977), Sissons and Dawson (1981), and Stoker et al. (2009) were used as a basis for identifying raised marine shorelines and deltas (Table 1). Raised marine feature elevations were surveyed using a Leica 1200 differential GPS, with a precision error of 0.1 m. The elevations of the geomorphic feature and sample burial depths were also measured. For constraining RSL, we used the elevation of the top of the delta, beach plain, or terrace. The elevation of the feature's top was adjusted for its indicative meaning using the indicative meaning calculator of Lorsheid and Alessio et al. (2019). Following Lorsheid and Alessio et al. (2019), paleo RSL was calculated by subtracting the reference water level, RWL, from the feature's observed elevation using Eq. 1:

$$Paleo\ RSL = observed\ elevation - RWL \tag{1}$$

where RWL represents the average of the upper and lower limits of formation (Eq. 2).

$$RWL = \frac{upper\ limit + lower\ limit}{2} \tag{2}$$

The paleo RSL error accounted for a precision measurement error of 10 cm from the differential GPS and the uncertainty of the modern analog, IR (Eq. 3).

$$Paleo\ RSL\ error = \sqrt{\left(\frac{IR}{2}\right)^2 + \left(\frac{measurement\ precision}{2}\right)^2} \tag{3}$$

IR is the indicative range defined as the range between the upper and lower limits of the RSL indicator formation (Eq. 4).

$$IR = upper\ limit - lower\ limit \tag{4}$$

Indicator	**Upper Limit**	**Lower Limit**
Raised Beach	Swash Height (SWSH)	Ordinary Berm (Ob)
Delta	Ordinary Berm (Ob)	Wave Breaking Depth (db)

Table 2. List of sea-level indicators and descriptive limits (from Lorsheid and Alessio et al. (2019)).

For raised beaches, RWL was approximated using the storm wave swash height (SWSH) as the upper limit, and the ordinary berm (Ob) as the lower limit. SWSH was calculated using Mean Higher High Water (MHHW) along with 2 standard deviations above the mean values for the deepwater significant wave height (H_s) and the deepwater wave length (L_0) (Eq. 5).

$$SWSH = 1.1\left(0.35s\sqrt{H_sL_0} + \frac{\sqrt{H_sL_0(0.563s^2+0.004)}}{2}\right) + MHHW \tag{5}$$

L_0 was calculated using the mean deepwater wave period (T_p) as proposed by Stockdon et al. (2006) (Eq. 6):

$$L_0 = \frac{g(T_p)^2}{2\pi} \tag{6}$$

Ob was approximated using the same equation as SWSH, but utilizing the mean values of H_s and L_0 rather than 2 standard deviations above their mean (Eq. 7). This equation (Eq. 7) adds the run-up of waves to the MHHW to account for run-up during regular high tides:

$$Ob = 1.1\left(0.35s\sqrt{H_sL_0} + \frac{\sqrt{H_sL_0(0.563s^2+0.004)}}{2}\right) + MHHW \tag{7}$$

For deltas, RWL was defined using Ob as the upper limit and the breaking depth of waves (db) as the lower limit. The lowest point of interaction between sediment and water, db, was determined using s, the beach slope, along with the mean values of L_0 and H_s (Eq. 8).

$$db = L_0(3.86s^2 - 1.98s + 0.88)\left(\frac{H_s}{L_0}\right)^{0.84} \tag{8}$$

3.2 Field Sampling

Uplifted marine deposits were sampled under a light-proof tarpaulin or using opaque tubes, depending on the grain size of the deposit, and wrapped in light-proof black plastic for transport to the laboratory. Dose-rate samples were collected from all distinct stratigraphic layers within 40 cm above and below the sample. The sedimentary section at each sample location was also described and logged.

During sampling, geomorphic features were identified using their general geomorphic characteristics and sedimentary structures. Raised beach plains mainly contained parallel laminations and/or ripple cross laminations and formed benches parallel to the modern coast. Stratigraphic sections within deltas contained interbedded muds and sands, often displaying a coarsening upwards profile. Stratigraphic descriptions of each sample site can be found in supplementary material.

Sample Number(s)	Latitude	Longitude	Sample Elevation m OD	Observed Elevation m OD	RSL Elevation m	RSL Elevation Error m	Location Name	Interpretation	Section Description	Source
KQ22-01/02/05	57.26950	-5.770713	Not measured	Not measured	Not measured	Not measured	Kyleakin	Delta	66-100 cm fine to coarse sand	Peach et al. (1910), Anderson and Dunham (1966)
TB22-01/02/03	57.3375	-6.109444	10.9	22.9	22.0	2.4	The Braes	Delta	35-80 cm laminated fine to cobbly sand	Walker et al. (1988)
^ STR22-02	57.26921	-5.973607	5.5	10.9	10.0	2.5	Strollamus	Beach Plain	70 cm gravelly sands	Ballantyne et al. (2010)
AP22-02/04	57.44461	-5.81518	14.5/18.1	20.4	20.0	2.0	Applecross Heritage Center	Beach Plain	26-46 cm cross-bedded medium to fine sand	Robinson (1977)
AP22-08	57.35314	-5.598103	24.6	27.1	26.2	2.4	Ardaneaskan	Beach Plain	53 cm cobbly fine sand	Robinson (1977)
AP22-11/12	57.55367	-5.840091	17.3/14.4	20.0	19.6	1.9	Cuaig Delta	Delta	212 cm fine to coarse sands with sedimentary structures	Robinson (1977)
AP22-14	57.52524	-5.597598	Not measured	Not measured	Not measured	Not measured	Shieldaig	Delta	40 cm gravelly coarse sand	This study
GA22-01/02/03	57.67487	-5.788722	18.4/17.9/18	20.9	20.9	0.1	Erradale	Fluvial Terrace	170 cm interbedded sorted fine to medium sand with gravels	Sissons and Dawson (1981)
GA22-06	57.64202	-5.802352	19.9	22.4	22.0	1.9	Redpoint	Beach Plain	140 cm interbedded cobbly gravels and ripple-cross laminated sands	Sissons and Dawson (1981)
* GA22-07	57.83558	-5.68529	10.4	15.0	11.8	0.5	Firemore Beach	Beach Plain	79 cm sorted sands and gravels	Sissons and Dawson (1981)
^ GA22-09/10	57.7412	-5.768652	10.0/10.8	13.4	13.0	1.9	Sands Caravan Park	Delta	10 m sandy and gravelly foresets	Sissons and Dawson (1981)
*GA22-16	57.86092	-5.4978	19.9	20.8	20.0	2.4	Second Coast	Beach Plain	180 cm well-bedded cobbly and gravelly sands	Sissons and Dawson (1981)
* GA22-17	57.89725	-5.384645	14.4	16.6	16.6	2.2	Badluarach	Beach Plain	80 cm well-bedded sands and gravels	Sissons and Dawson (1981)
* UL22-01	57.87472	-5.130556	12.6	12.6	12.3	1.9	Loggie	Delta	172 cm bedset of interbedded sandy gravels and sands	Stoker et al. (2009)
* UL22-03	57.89939	-5.167714	12.2	14.7	14.7	1.6	Ullapool	Outwash Delta	87 cm sands and gravels	Stoker et al. (2009)
* UL22-04	58.02682	-5.357896	11.3	13.6	12.8	2.4	Achiltibuie	Beach Plain	72 cm planar bedded sands and gravels	Stoker et al. (2009)

^ Not the highest shoreline feature in the sequence

* Inside WRR

Table 1. Locations of sites sampled in this study along with their elevations, interpreted sedimentary landform, and the original publications where each site was mapped.

3.3 OSL Sediment Processing

Quartz extracts, ranging between 63 and 250 µm, from the collected samples were prepared in a dark room under subdued red-light conditions. Quartz was chosen due to its abundance in the sediments and known stability of luminescence emissions. Where opaque tubes had been used for sampling, about 2-3 cm of light-exposed material from each end were discarded. Samples were sieved, treated with 3.75% HCl to remove carbonates, and 27% H_20_2 to remove organics. Density separations using lithium heteropolytungstate (LST) with densities of 2.62 and 2.75 g/cm^3 were performed to isolate and separate quartz and feldspars, then sieved once more to narrow the grain size fraction. To remove feldspar contamination and eliminate the surface shell affected by alpha radiation, which penetrates the outer 20-30 µm of the grains (Aitken, 1998; Wagner, 1998), samples were etched with 48% HF for 40 minutes (Fleming, 1979). Three millimeter quartz aliquots were prepared on stainless steel discs using silicone spray for measurement.

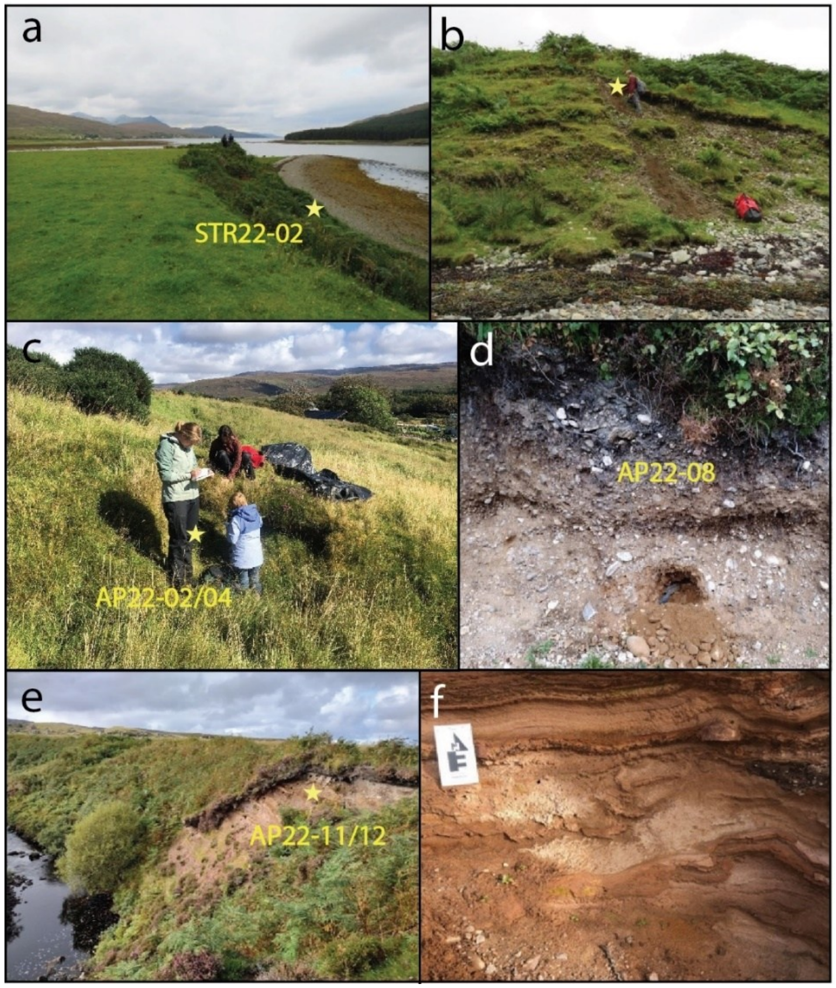

Figure 2. Photographs of sample sites from Strollamus and Applecross. (a) (b) Sample STR22-02 from a raised beach plain in Strollamus. This raised beach plain is the middle of a sequence of three raised features. (c) Samples AP22-02 and AP22-04 from a beach plain located near the Applecross Heritage Center. (d) Sample AP22-08 from a raised beach plain in Ardaneaskan**.** (e) Samples AP22-11 and AP22-12 from the Cuaig Delta. (f) The Cuaig Delta section displaying well-bedded sands (and gravels) with fluid-escape features.

Figure 3. Photographs of sample sites near Gairloch. (a) Samples GA22-01, GA22-02, and 03 extracted from an uplifted fluvial terrace located in Erradale. (b) A section (where sample GA22-01 was extracted) from the raised beach plain in Erradale containing swaley cross-stratification within the marine deposits. (c) A section featuring ripple cross laminations from a beach plain located at Redpoint. (d) Sample GA22-06 from a beach plain located at Redpoint. (e) Sample GA22-07 from Firemore beach. (f) A section from

Firemore beach plain containing crossbedded coarse to medium sand. (g) A section from a delta located at Sands Caravan Park. (h) Samples GA22-09 and GA22-10 from a delta located at Sands Caravan Park. (i) Sample GA22-16 from a raised beach plain located at Second Coast. (j) Sample GA22-17 from a raised beach plain in Badluarach.

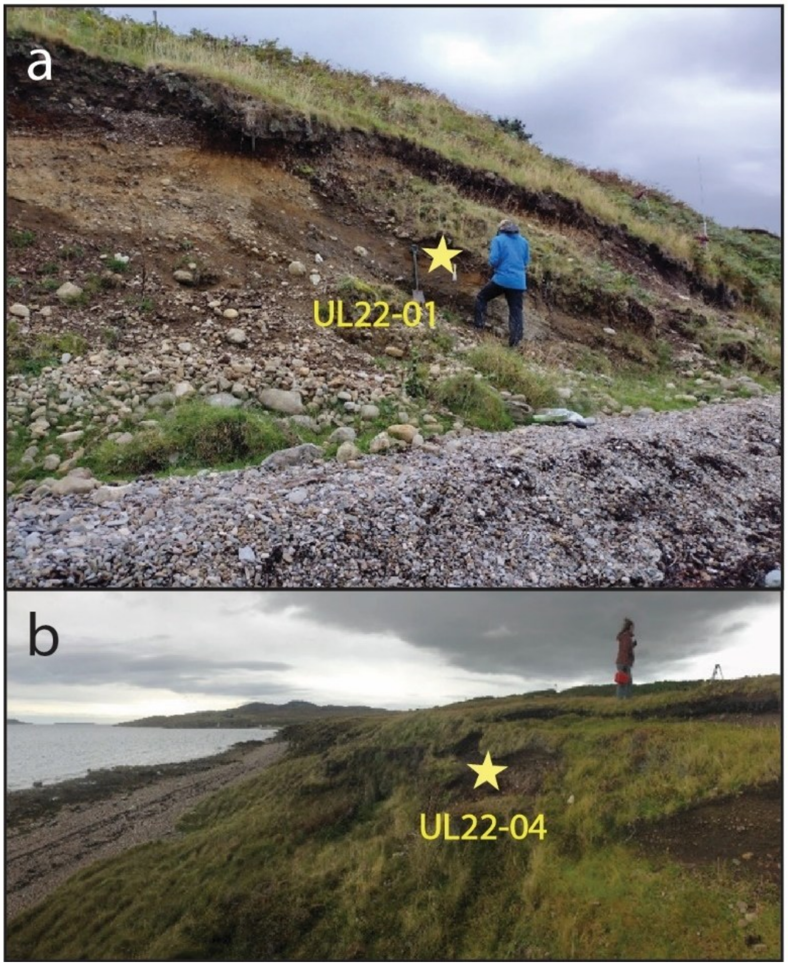

Figure 4. Photographs of sample sites from Ullapool. (a) Sample UL22-01 from a delta located in Loggie. (b) Sample UL22-04 from a raised beach plain in Achiltibuie.

3.4 OSL Measurements

OSL measurements were conducted using a Risø TL/OSL-DA-20 reader, Risø National Laboratory, with a built-in $^{90}Sr/^{90}Y$ beta source giving an internal beta source dose rate of approximately 100 mGy/s. The exact dose rate was determined for each individual measurement. Optical stimulation was carried out with blue LEDs (470 nm, 82 mW/cm^2) and infrared stimulation with an IR LED array (875±80 nm, 124 mW/cm^2) using a Hoya U-340, 290-370 nm detection filter.

The equivalent dose was determined for each sample, once quartz and feldspars were separated, using a single-aliquot regenerative dose (SAR) procedure on small aliquots (3 mm) (Murray and Wintle, 2000; Wintle and Murray, 2006). The central age model was used to determine equivalent dose as it may be applied when aliquots have received the same or different doses (Galbraith, 1999; Galbraith and Roberts, 2012).

The total dose rate or environmental dose rate was determined by estimating the exposure of mineral grains to ionizing radiation from the decay of ^{238}U and ^{232}Th series and ^{40}K, and cosmic sources during the burial period. Attenuation by water, and contributions from beta radiation and gamma radiation are taken into account. Water content was measured from the wet and dry weight of samples as water in the pore space between beach sediment absorbs radiation and reduces the effective dose rate. The samples were nearly dry with the water content for each sample, measuring approximately 1-2%. The ^{238}U and ^{232}Th series and ^{40}K nuclide concentrations were estimated using high-resolution gamma spectrometry with conversion factors by Guérin et al. (2011). The cosmic ray dose rate was determined as described in Prescott and Hutton (1994), based on the intensity vs. depth relation for muons given by Barbouti and Rastin (1983). Following the calculations of the equivalent and total dose rates, the age of each sample was determined by dividing the equivalent dose by the total dose rate.

4. Results

4.1 Elevation of the Lateglacial Shoreline

Similar to previous studies (McCann, 1966; Sissons, 1976; Sissons and Dawson, 1981), a general decrease in elevation of the Lateglacial shoreline to the north was observed (Table 1, Fig. 5). Outside the WRR limits, the highest observed shoreline was at Ardaneaskan with an elevation of 26.2 ± 2.4 m and the lowest was at Greenstone Point near Gruinard Bay with an elevation of 18.0 ± 0.4 m (Sissons and Dawson, 1981). In addition, shorelines were on average lower inside the limits of the WRR (~15.5 m) than outside the WRR (~22.1 m) (Table 1, Fig. 6).

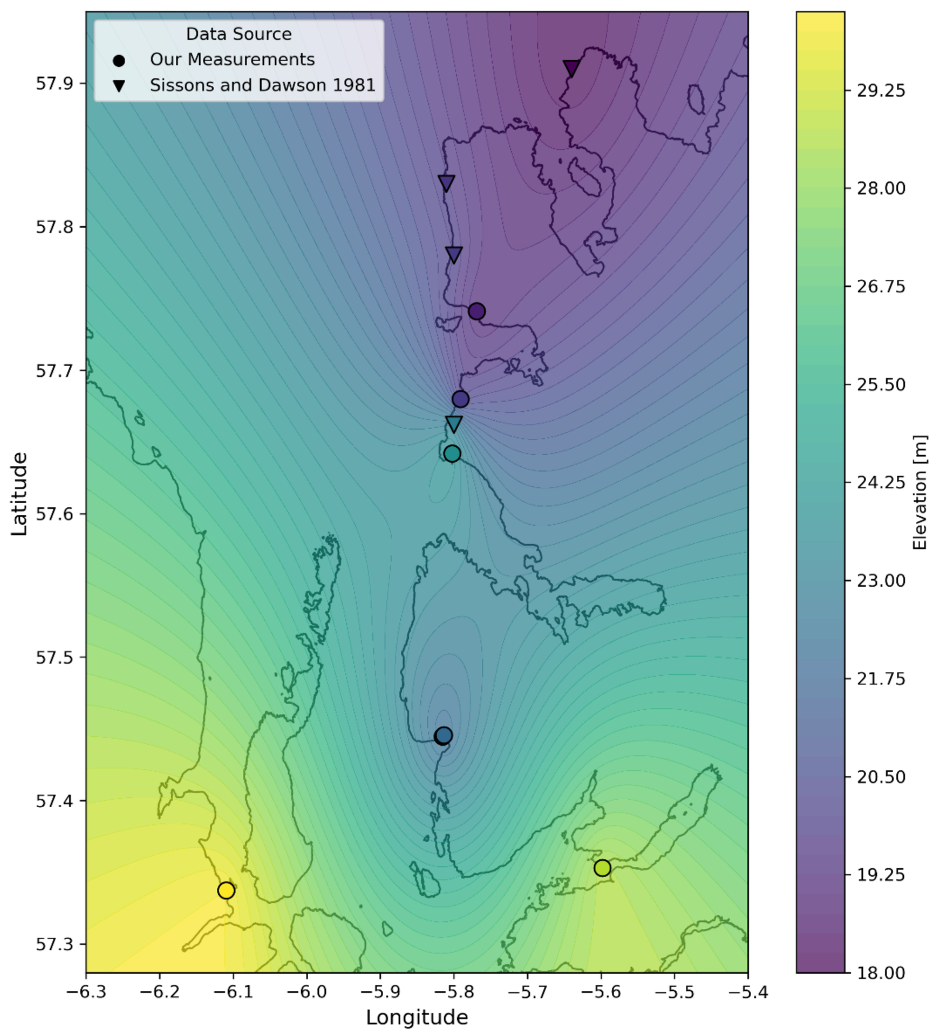

Figure 5. Elevation map of the Lateglacial shoreline defined with RSL elevations (observed elevation measurements adjusted for their indicative meaning) from Sissons and Dawson (1981) and those presented in this study and the supplementary material. All elevations outside of the WRR boundary were used for Kriging interpolation over a mesh grid to estimate RSL between known elevations.

Sample	Location	Feature	RSL Elevation	RSL Elevation Error	Crystal size (µm)	Aliquot	Equivalent Dose (Gy)	Dose error (Gy)	OvD (%)	Dose rate (Gy/ka)	Dose rate error (Gy/ka)	Age (ka)	Age error (ka)
STR22-02	Strollamus	Beach Plain	10.0	5.0	180-212	25	40.0	2.7	9	2.943	0.100	13.6	2.0
AP22-02	Applecross Heritage Center	Beach Plain	20.0	4.0	150-180	38	49.6	2.7	9	2.677	0.010	18.5	2.4
AP22-04	Applecross Heritage Center	Beach Plain	20.0	4.0	150-180	26	46.3	2.7	0	2.510	0.115	18.5	2.8
AP22-08	Ardaneaskan	Beach Plain	26.2	4.8	90-125	27	52.6	4.1	24	2.575	0.090	20.4	3.4
AP22-11	Cuaig Delta	Delta	19.6	3.8	180-212	26	48.0	2.8	8	2.521	0.082	19.0	2.6
AP22-12	Cuaig Delta	Delta	19.6	3.8	90-125	38	64.0	3.6	11	3.012	0.103	21.2	2.8
GA22-01	Erradale	Fluvial Terrace	20.9	0.1	125-150	29	55.1	3.2	8	2.535	0.087	21.7	3.0
GA22-02	Erradale	Fluvial Terrace	20.9	0.1	150-180	24	58.1	3.7	15	2.285	0.074	25.4	3.6
GA22-03	Erradale	Fluvial Terrace	20.9	0.1	150-180	22	59.6	3.7	14	2.070	0.071	28.8	4.0
GA22-06	Redpoint	Beach Plain	22.0	3.8	150-180	26	79.9	5.4	17	2.671	0.086	29.9	4.6
GA22-07	Firemore Beach	Beach Plain	11.8	1.0	125-150	31	35.7	2.2	14	1.931	0.063	18.5	2.6
GA22-09	Sands Caravan Park	Delta	13.0	3.8	150-180	29	42.9	2.3	0	2.493	0.086	17.2	2.2
GA22-10	Sands Caravan Park	Delta	13.0	3.8	180-212	26	42.8	2.6	5	2.343	0.073	18.3	2.4
GA22-16	Second Coast	Beach Plain	20.0	4.8	250-300	46	29.9	1.7	9	1.821	0.066	16.4	2.2
GA22-17	Badluarach	Beach Plain	16.6	4.4	150-180	27	39.8	2.3	3	2.163	0.070	18.3	2.4
UL22-01	Loggie	Delta	12.3	2.8	90-150	24	84.1	7.1	19	3.304	0.095	25.5	4.6
UL22-04	Achiltibuie	Beach Plain	12.8	4.8	180-212	34	38.7	2.4	12	2.647	0.085	14.6	2.0

Table 3. Summary of OSL ages. Aliquot is the number of aliquots that passed the reliability tests of the SAR procedure and were used for calculation of the equivalent dose. Doses were calculated using the central age model of Galbraith et. al. (1999); OvD represents the overdispersion value from the model which describes the width of the distribution. All errors are 2 sigma.

4.2 OSL Dates and Geomorphic Interpretations Progressing Northward

4.2.1 Isle of Skye OSL

We attempted to date the Lateglacial shoreline at 3 locations along the NE coast of the Isle of Skye Kyleakin, Strollamus, and the Braes. The Braes is underlain by basalt; Strollamus is underlain by granite; and Kyleakin is underlain by Torridonian Sandstone.

The three samples (KQ22-01, KQ22-02, KQ22-05) collected from the base of a ~15 m thick series of outcrops within a quarry in a raised delta in Kyleakin, were obtained from three different sedimentary sections, a 100 cm bed of find sand, a 66 cm bed of coarse to fine sand, and an 85 cm bed of fine to medium sand. Initial attempts using quartz were unsuccessful, so feldspar dating was attempted instead. The three feldspar samples returned ages between ~111-178 ka (Table 1).

At the Braes, Walker et al. (1988) identified a raised shoreline, with an elevation of ~30 m OD along a raised tombolo, as the Lateglacial marine limit. That shoreline dips to the Northeast toward the straight between Skye and Raasay where we sampled two locations of a raised delta whose top elevation was 22 ± 2.4 m OD. The first, a 35 cm section of cobbly sand on the east side of the delta, returned an age of 77 ka (TB22-01). Two other ages of 93 ka and 47 ka from samples TB22-02 and TB22-03 were obtained from an 80 cm sedimentary section on the west side of the delta containing thin beds of laminated fine sand, medium and coarse sand, and cobbly sand.

Ballantyne et al. (2010) mapped the highest Lateglacial shoreline at Strollamus to be ~23 m OD. Sample STR22-02 was taken from the second highest constructional bench at Strollamus, interpreted as a beach plain, in a sequence of 3 benches (Fig. 2a). The shore-parallel feature had a bench top elevation of 10.9 ± 0.1 m OD. Adjusting for its indicative meaning resulted in a RSL elevation of 10.0 ± 2.5 m. The 70 cm bed at an elevation of 5.5 ± 0.1 m OD consisted of gravelly sands (Fig. 2b). The single sample obtained from the section returned an age of 13.6 ± 2 ka.

4.2.2 Applecross OSL

Progressing northeastward, on and adjacent to the Applecross Peninsula, we attempted dating of raised marine features at Ardaneaskan, Applecross Heritage Center, the Cuaig Delta, and East Shieldaig (Fig. 1). Sample AP22-14 from a fluvial terrace east of Shieldaig returned a relatively old age of 150 ± 9.6 ka, while samples from the Applecross Heritage Center, Ardaneaskan, and Cuaig Delta returned younger post-glacial ages.

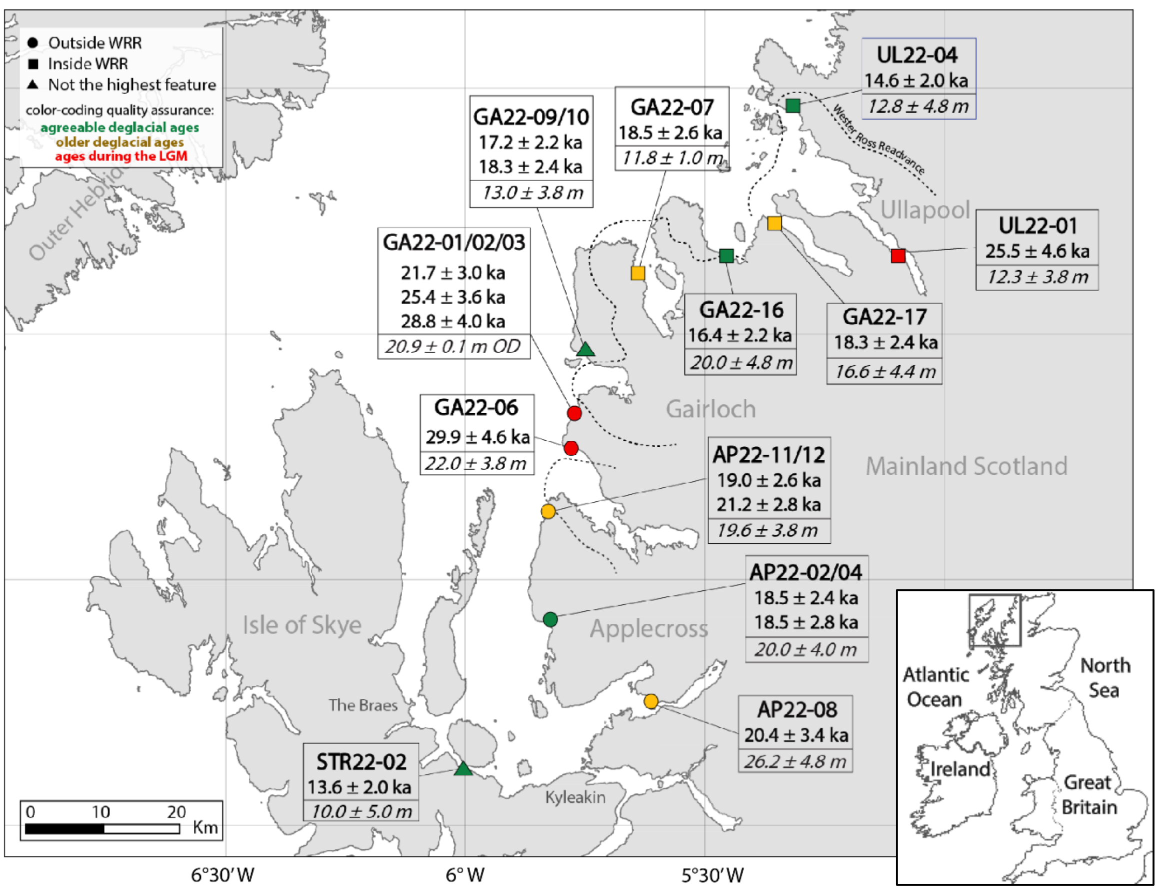

Figure 6. OSL dated raised marine deposits with their respective RSL elevations corrected for their indicative meaning. Samples denoted with a square are located inside the Wester Ross Readvance Boundary limits (drawn with a dotted line) mapped in full by Robinson and Ballantyne (1979), Sissons and Dawson (1981), Ballantyne et al. (2009), Ballantyne and Stone (2012), Ballantyne and Bradwell

(2021), Bradwell et al. (2021), and Bradwell and Stoker et al. (2023). While samples with a circle are outside of the WRR boundary. Triangular shaped points are samples outside the WRR boundary but obtained from the second highest geomorphic feature. Dates are in kiloyears, and elevation is in meters. Quality assurance of samples identified by color are discussed in section 5.1. Their location inside or outside the WRR boundary is taken into consideration in the quality assessment.

Near Ardaneaskan, located southeast of the Applecross Peninsula (Fig. 1), Robinson et al. (1977) mapped a marine terrace with an elevation of ~30 m OD. Similarly, we sampled (AP22-08) a matrix-supported cobbly stiff fine tan sand associated with a broad bench, interpreted as a beach plain, at an elevation of 27.1 ± 0.1 m OD. Adjusting for its indicative meaning suggests an RSL elevation of 26.2 ± 2.4 m. Sample AP22-08 was extracted from a 53 cm section of stiff cobbly fine sand within a bench at an elevation of 24.6 ± 0.1 m OD (Fig. 2d). The gravelly sand is cross-bedded with no mud content and the cobbles are very well rounded, suggesting a marine origin. The sample returned an age of 20.4 ± 3.4 ka.

North of Ardaneaskan, Applecross village is located at the head of a small fjord, which is formed by the flooding of a small tributary valley of the Minch. Robinson et al. (1977) mapped a bench on the western side of this fjord. A similar feature is found on the eastern side of the fjord where we collected two samples (AP22-02, AP22-04) 150 m apart (Fig 2c). The geomorphic feature sampled was a constructional sandy bench running parallel to the modern shoreline with a top elevation of 20.4 ± 0.1 m OD interpreted as a beach plain. Adjusting for its indicative meaning suggests an RSL elevation of 20.0 ± 2.0 m. The first, sample AP22-02 at an elevation of 14.5 ± 0.1 m OD from a 46 cm thick exposure of cross-bedded medium to fine sand within the 200 m long bench, returned an age of 18.5 ± 2.4 ka. The second, sample AP22-04 at an elevation of 18.1 ± 0.1 m OD obtained from a 26 cm thick exposure of bedded fine to medium sand, returned an age of 18.5 ± 2.8 ka.

At the Cuaig Delta, samples AP22-11 and AP22-12 were extracted from a 212 cm sedimentary section near the community of Cuaig (Fig. 2e). The section is well exposed in a cutbank of Abhainn (River) Chuaig and consists of interbedded sands, muds, and gravels with parallel laminations, ripple cross-laminations, trough cross-bedding, drop stones, fluid-escape structures, and soft-sediment deformation (Fig. 2f). The delta is inset into a marine platform mapped by Robinson et al. (1977) at an elevation of 26.8 m OD. The topset of the delta attains an elevation of 20.0 ± 0.1 m OD with an RSL elevation of 19.0 ± 1.9 m when adjusted for its indicative meaning. Samples AP22-11 and AP22-12 collected at elevations of 17.3 ± 0.1 m OD and 14.44 ± 0.1 m OD (one below the other) returned ages of 19.0 ± 3.4 ka and 21.2 ± 2.8 ka, respectively. A third sample (AP22-13) at a lower elevation of an adjacent section returned an age of ~150 ka at an elevation of 11.4 ± 0.1 m OD.

East of Shieldaig is a broad elevated terrace cut by the River Balgy, an outlet stream from Loch Damh. The terrace lies at an elevation between 15-19 m OD. A ~40 cm pit was excavated into a cutbank of the terrace. The gravelly coarse sand yielded an age of 150 ± 9.6 ka.

4.2.3 Gairloch OSL

Farther north in Wester Ross near the community of Gairloch, 6 sites were sampled and dated: Redpoint, Erradale, Sands Caravan Park, Firemore Beach, Second Coast, and Badluarach (Fig. 3). Several marine features including a well-developed tombolo were observed at Redpoint and mapped by Sissons and Dawson (1981). Along a beach cliff, cut into the highest of these marine features, is a section containing interbedded sorted fine to medium sand and well-rounded gravels (Fig. 3d). The sand beds have wavy bedding planes as well as oscillation ripple cross-laminations (Fig. 3c). The interpreted raised beach plain deposits extend to a top elevation of

22.4 ± 0.1 m OD, similar to Sissons and Dawson (1981)'s reported elevation of 23.5 m OD, and after adjusting for its indicative meaning, results in an RSL elevation of 22.0 ± 1.9 m. Sample GA22-06, extracted from a 140 cm section of interbedded cobbly gravels and ripple-cross laminated sands at an elevation of 19.9 ± 0.1 m OD, returned an age of 29.9 ± 4.6 ka.

Near the community of Erradale is an elevated fluvial terrace of sands and gravels inset into a shingle ridge at an elevation of 21.0 m OD mapped by Sissons and Dawson (1981) (Fig. 3a). A sediment exposure within the terrace contains cross stratified sands and gravels (Fig. 3b). Three samples were extracted; GA22-01, GA22-02, GA22-03, at elevations of 18.37 m OD, 17.9 ± 0.1 m OD, 18.0 ± 0.1 m OD and returned ages of 21.7 ± 3.0 ka, 25.4 ± 3.6 ka, 28.8 ± 4.0 ka, respectively. We surveyed the top of the terrace at 20.9 ± 0.1 m OD. As the fluvial terrace likely graded to sea level, it provides an upper limit to RSLs at the time.

At Sands Caravan Park, a shore parallel bench interpreted as the Lateglacial shoreline at an elevation of 18.4 ± 0.1 m OD with an RSL of 18.1 ± 1.9 m is incised into by another series of 1-2 lower lying benches with a planform shape of a delta. Sissons and Dawson (1981) mapped the higher bench as a raised shoreline with an elevation of 20.6 m. The highest of the two inset lower benches is cut by the River Sand, exposing a 10 m high section of sandy and gravelly foresets (Fig. 3h). Two samples (GA22-09, GA22-10) were collected from the sandy foresets of this interpreted delta (Fig. 3g). The top of this raised delta has an elevation of 13.4 ± 0.1 m OD with an RSL elevation of 13.0 ± 1.9 m after adjusting for its indicative meaning. Samples GA22-09 and GA22-10 at elevations of 10.0 ± 0.1 m OD and 10.76 ± 0.1 m OD returned ages of 17.2 ± 2.2 ka and 18.3 ± 2.4 ka, respectively (Fig. 3d).

North of Sands, at Firemore beach (GA22-07) in the vicinity of a shingle ridge mapped by Sissons and Dawson (1981) at an elevation of 16.4 m OD, is a well-developed bench running parallel to the shoreline composed of sorted sands and gravels (Fig. 3e). On the north side of the beach, the bench is cut by a small creek on one side and the sea cliff on the other. Sediment exposed within the bench displays three sedimentary units. The upper bedset is composed of well-rounded cobbles and other clasts up to boulder size, overlying a black-brown sand with some well-rounded cobbles and in some locations displaying wavy bedding (Fig. 3f), and a lowermost bedset of lighter color with faintly developed planar laminations and a lower proportion of gravel. The bench has a top elevation of 14.6 ± 0.1 m OD. Correcting for its indicative meaning gives an RSL elevation for the feature of 11.8 ± 0.5 m. One sample (GA22-07) collected at an elevation of 10.4 ± 0.1 m OD from a 79 cm section of the lower bedset containing laminations of coarse sand and gravel, yielded an age of 18.5 ± 2.6 ka. Another sample (GA22-08) was obtained from a better developed beach on the north side of headland north of Firemore beach; this sample returned an age of ~176 ka.

Another shore-parallel bench with an elevation of 20.8 ± 0.1 m OD was sampled at Second Coast near the location of a shoreline mapped by Sissons and Dawson (1981) at an elevation of 20.1 m OD. The constructional bench is composed of well-bedded cobbly and gravelly sands with well-rounded gravels up to cobble size. Some low-angle cross-bedding is also present within the deposits interpreted as a raised beach plain (Fig. 3i). Sample GA22-16 was taken from one of the beds at an elevation of 19.9 ± 0.1 m OD and produced an age of 16.4 ± 2.2 ka, despite containing a larger quartz size (250-300 μm) not ideally suited for OSL dating. We assign an RSL elevation for this site of 20.0 ± 2.4 m.

Our most northern sample in the Gairloch region, GA22-17, is located in Badluarach near the location of a raised shoreline at an elevation of 17.0 m OD mapped by Sissons and Dawson (1981). Similar to the site at Second Coast, it was collected from a shore-parallel bench composed of well-bedded sands and gravels (Fig. 3j). The bench was much more extensive than at Second Coast extending another 1.1 km to the NW and another 2.7 km to the SE of our sample site. It is interpreted as a raised beach plain with a top elevation of 16.6 ± 0.1 m OD. Adjusting for its indicative meaning results in a RSL elevation of 16.6 ± 2.2 m. The sample collected from a pit dug into the bench at an elevation of 14.4 ± 0.1 m OD, GA22-17, returned an age of 18.3 ± 2.4 ka.

4.2.4 Ullapool OSL

Two sites were sampled in the Ullapool region, Loggie and Achiltibuie (Fig. 4). At the head of Little Loch Broom, opposite the town of Ullapool, a well-developed pair of benches are present; the higher of the two benching being interpreted by Stoker et al. (2009) as a fan delta. The higher bench is composed of steeply dipping foresets composed of sands and gravels similar to the classic Gilbert Deltas developed in other regions. The interpreted raised delta has a topset surface elevation of 12.6 ± 0.1 m OD. Sample UL22-01 was collected at an elevation of 7.3 ± 0.1 m OD from a 172 cm thick bedset containing interbedded sandy gravels and sands (Fig. 4a) and returned an age of 25.5 ± 4.6 ka. Adjusting for indicative meaning, this delta represents an RSL elevation of 12.3 ± 1.9 m.

The second sample (UL22-04) collected from the Ullapool region was from a shore-parallel bench near the village of Achiltibuie composed in some places of eroded till and in other places of alternating planar bedded sands and gravels (Fig. 4b). The interpreted beach plain has a top elevation of 13.6 ± 0.1 m OD returning a RSL elevation of 12.8 ± 2.4 m. From this uplifted beach plain, an OSL sample from the interbedded sands and gravels, at an elevation of 11.3 ± 0.1 m OD, returned an age of 14.6 ± 2.0 ka.

4.3 Intrasite Comparison of Ages

Most samples taken from the same sites yielded the same age within error. At Applecross Heritage Center, samples taken 150 m apart across the same feature at an elevation, adjusted for its RSL indicative meaning (RSL IM), of 20.0 ± 2.0 m yielded congruent ages within error (AP22-02, 18.5 ± 2.4 ka; AP22-04, 18.5 ± 2.8 ka). Similarly, two of the three samples extracted from the Cuaig Delta at an elevation of 19.0 ± 1.9 m (RSL IM) yielded ages within error of one another (AP22-11, 19.0 ± 3.4 ka; AP22-12, 21.2 ± 2.8 ka). Two samples extracted from a delta located at Sands Caravan Park with an elevation of 13 ± 1.9 m (RSL IM) also returned ages within error range of each other (GA22-09, 17.2 ± 2.2 ka; GA22-10, 18.3 ± 2.4 ka). However, the three samples taken from a fluvial terrace at an elevation of 20.5 ± 1.9 m (RSL IM) in Erradale returned more variable ages (GA22-01, 21.7 ± 3.0 ka; GA22-02, 25.4 ± 3.6 ka; GA22-03, 28.8 ± 4.0 ka). Two of these samples, GA22-01 and GA22-03, returned ages not within error despite being extracted from the same geomorphic feature.

5. Discussion

5.1 OSL Characteristics and Age Reliability

Out of the 26 samples targeted for dating, 9 produced ages significantly older than the LGM (approximated by Peltier and Fairbanks (2006) to be ~19-26.5 ka), while 4 returned ages corresponding to the LGM. Four other samples yielded deglacial ages but older than previous models for deglaciation in the region, and two additional samples located inside the WRR boundary also returned deglacial ages older than previously published estimates. Seven samples returned ages that broadly agree with the prevailing models for the region’s deglacial history (Gowan et al. 2021; Tarasov et al. 2012; Bradley et al. 2023).

5.1.1 Significantly Old OSL Ages

Nine OSL samples returned ages that were significantly older than expected based on previously published estimates. These include three from Kyleakin, three from the Braes, and one each from the Cuaig Delta, Shieldaig, and a beach near Firemore.

At Kyleakin, the quartz grains from samples KQ22-01, KQ22-02, and KQ22-05, collected from a delta, showed insufficient luminescence signals, likely due to partial bleaching or low signal sensitivity, and thus were undatable. Feldspar grains yielded unexpectedly old ages ranging from ~111-178 ka. The stratigraphic feature at Kyleakin, which is over 15 meters thick, exhibits considerable stratigraphic variability with several bedsets separated by pronounced unconformities. Our samples were taken from the base of the section near its bedrock contact. Thus, the ages could be dating earlier phases of a large composite feature reworked or reoccupied multiple times. Alternatively, the sand grains may have not been completely reset.

Samples TB22-01/02/03 from the Braes displayed significant disequilibrium in the uranium decay chain, as all three samples exhibit higher concentrations of ^{238}U than ^{234}U. This suggests the loss of ^{234}U, which would result in a lower dose rate and, consequently, an overestimated age (Olley et al. 1996). These samples also contained relatively high dispersion, which could suggest incomplete reset or grain mixing, which may also account for their unexpectedly old ages (~47 to 93 ka). Additionally, the deposits at the Braes are ~ 20m thick and we were only able to observe the lower portions of the feature. Thus, it too could potentially represent a composite feature.

Sample AP22-13 from the Cuaig Delta contained some aliquots with signal saturation, meaning that the natural luminescence signal reached a maximum value, beyond which it could no longer increase. This saturation likely resulted in an underestimated age of ~150 ka. This old age, from much lower in the section, might suggest this represents an older part of the deposit or the grains simply were not fully reset.

Samples AP22-14, from Shieldaig, and GA22-08, from a beach near Firemore, both displayed no anomalous OSL properties, yet returned older-than-expected ages of ~105 ka and ~177 ka, respectively. In the field, no evidence suggested that these samples were taken from composite features. Thus, potentially they were never fully reset. Given the anomalously old ages of these samples in comparison to previously published estimates and other samples presented here, these nine samples were excluded from further analysis in this work.

5.1.2 Ages during the LGM

Four samples, UL22-01, GA22-02, GA22-03, GA22-06, returned anomalously old ages falling between 25.4 and 29.9 ka, a time in which the region was thought to be covered by ice (Ballantyne 2010; Bradwell et al. 2019, 2021). These samples exhibited luminescence characteristics (i.e. IR signal depletion) suggesting potential feldspar contamination due to inadequate density separation of feldspar and quartz during the OSL preparation. Consequently, these samples from Erradale (GA22-02, GA22-03), Redpoint (GA22-06), and Loggie (UL22-01) with ages 25.4 ± 3.6 ka, 28.8 ± 4.0 ka, 29.9 ± 4.4 ka, and 25.5 ± 4.6 ka are likely post-glacial; however, the contamination limits their reliability, preventing further meaningful interpretations.

5.1.3 Older Deglacial Ages for the MnIS

The oldest deglacial OSL ages outside of the WRR were obtained from Erradale (GA22-01), Ardaneaskan (AP22-08), and the Cuaig Delta (AP22-11, AP22-12). These samples returned significantly older ages (21.7 ± 3.0 ka, 20.4 ± 3.4 ka, 19.0 ± 2.4 ka, 21.2 ± 2.8 ka) compared to the rest, but given their large uncertainties do fit within error of when MnIS deglaciation probably began ~18.5 ka (Gandy et al. 2018; Bradwell et al. 2019; Clark et al. 2022), suggesting they may date to the initial retreat of the ice stream from the Minch. However, none of the samples had particularly good OSL characteristics. Sample GA22-01 from Erradale, with an age of 21.7 ± 3.0 ka, may have been affected by disequilibrium in the uranium decay chain as it has low thorium and high uranium levels, which may increase the influence of uranium on the age determination.

Sample AP22-08, extracted from Ardaneaskan, exhibited strong feldspar contamination and relatively high overdispersion at 24%. Overdispersion values exceeding 20% may indicate grain mixing or partial solar resetting (Arnold and Roberts, 2009). Thus, although this age of 20.4 ± 3.4 ka is congruent within error of other samples from the Applecross Peninsula, it is likely too old.

Samples AP22-11 and AP22-12 (both from the Cuaig Delta), with ages 19.0 ± 2.4 ka and 21.2 ± 2.8 ka, exhibited disequilibrium in the uranium decay chain as mentioned in section 5.1.1, which would result in a lower dose rate and an overestimated age. Additionally, since both samples were extracted from a delta, their high ^{234}Th concentrations could indicate freshwater flushing of the sediment, which may have removed ^{234}U and led to an artificially lower dose rate and therefore an older age (Aitken, 1998). However, there is speculation whether the Cuaig Delta is located inside the limits of the WRR despite being mapped outside by Ballantyne and Bradwell (2021).

5.1.4 Older Deglacial Ages for the WRR

Two samples within the WRR moraine boundary returned relatively old deglacial ages. Samples collected from Firemore (GA22-07) and Badluarach (GA22-17), exhibited good OSL characteristics (e.g. low dispersion, no disequilibrium, etc.) and returned post-glacial ages of 18.5 ± 2.6 ka and 18.4 ± 2.4 ka, respectively. These ages are slightly older than expected for shorelines within the WRR boundary, but still fall within the error range of some estimates of the WRR age. Additionally, sample GA22-17, from Badluarach, was collected from a shoreline thought to be within the WRR limits but without a clearly defined limit, raising the possibility that this sample actually lies just *outside* the WRR and thus represents an age for the marine limit *prior to* the WRR. However, the marine evidence (moraines and stratigraphy) in this area has been interpreted to suggest otherwise (Stoker et al. 2009).

5.1.5 Agreeable MnIS and WRR OSL ages

We identified seven OSL ages in reasonable agreement with previous work (Bradwell et al. 2008; 2019; 2021; Small et al. 2012; Simms et al. 2022). Of these, two samples from Second Coast (GA22-16) and Achiltibuie (UL22-04), both located within the WRR boundary, returned ages of 16.4 ± 2.2 ka and 14.6 ± 2.0 ka, respectively. Outside the WRR boundary, samples extracted from Strollamus (STR22-02), Applecross (AP22-02, AP22-04), and Sands (GA22-09, GA22-10) yielded ages of 13.6 ± 2.0 ka, 18.5 ± 2.4 ka, 18.5 ± 2.8 ka, 17.2 ± 2.2 ka, and 18.3 ± 2.4 ka, respectively. However, samples STR22-02, GA22-09, and GA22-10 were extracted from the second-highest geomorphic feature, which suggests that the marine limit at these locations is slightly older than these ages.

5.2 Age of Deglaciation in NW Scotland

5.2.1 Implications for Ice Sheet History

Even after removing the 13 samples interpreted to be too old, in addition to the 4 that are likely too old, our remaining 9 samples returned OSL ages older than previous models for the timing of the MnIS retreat and the WRR (Bradwell et al. 2019; 2021). In this area, Bradwell et al. (2021) showed that the retreat of the MnIS occurred rapidly between ~15.5-18.5 ka based on TCN ages from the onshore geomorphic equivalents of grounding zone wedges offshore. However, despite errors of ~2-3 ka, our mean OSL ages from the Applecross Heritage Center (AP22-02, AP22-04), Firemore Beach (GA22-07), Badluarach (GA22-17), and Sands Caravan Park (GA22-10) are older than 18 ka.

Our ages from Strollamus (STR22-02), Sands Caravan Park (GA22-09), Second Coast (GA22-16), and Achiltibuie (UL22-04) fall within error of previously published TCN ages of the timing of retreat (Bradwell et al. 2019, 2021; Small et al. 2012). For instance, Small et al. (2012) reported a ^{10}Be age of 14.3 ± 1.8 ka for a moraine at Strollamus, within close proximity (2 km) of sample STR22-02 with an age of 13.6 ± 2.0 ka. However, the beach we dated was not the highest beach, but rather the middle in a sequence of 3 beaches and thus the timing of ice retreat was likely a little earlier, but not by much given the rates of RSL fall experienced immediately after deglaciation. Similarly, a delta located at Sands Caravan Park contains an OSL age of 17.2 ± 2.2 ka (GA22-09) that falls within error of a ^{10}Be age on a glacial deposit located nearby with an age of 15.6 ± 1.4 ka reported by Ballantyne and Small (2019). However, the other OSL age from this deposit, 18.3 ± 2.4 ka (GA22-10), does not fall within error of the TCN age. Similar to Strollamus, the shoreline sampled at Sands Caravan Park is not the highest at that location and given high rates of RSL fall experienced immediately after deglaciation (Shennan et al. 2018), the age of the higher features is likely not much older than the ages from the slightly lower shorelines. We estimated the age of the highest bench located at Sands Caravan Park, which has an RSL elevation of 18.1 ± 1.9 m, using GIA modeled rates of RSL fall. The rate of RSL fall predicted for this time interval by the Bradley-Hybrid GIA model (Bradley et al. 2023) suggests an age of 18.6 ± 0.8 ka for the highest beach at Sands Caravan Park.

Within the Gairloch area, another sample, located at Second Coast (GA22-16), also exhibited an age, 16.4 ± 2.2 ka, within error of a ^{10}Be age on a glacial deposit, 15.3 ± 2.2 ka (Ballantyne and Small, 2019). Similarly, a raised beach in Achiltibuie (UL22-04) with an age of 14.6 ± 2.0 ka is situated near a ^{10}Be glacial deposit age of 15.2 ± 1.6 ka reported by Bradwell et al. (2008). However, these two samples (GA22-16, UL22-04) fall within the limits of the later WRR. Therefore, these two samples along with samples STR22-02 and GA22-09, which are also not from the highest bench in their respective sequences, are unlikely to accurately constrain the age of the MnIS retreat.

5.2.2 Rate of Retreat of the Minch Ice Stream

The former MnIS is thought to have undergone rapid retreat approximately 15.5-18.5 ka (Bradwell et al. 2019, 2021). However, some of our ages suggest that this rapid retreat may have begun earlier. After disregarding those OSL ages obtained from locations inside the WRR (Fig. 6) and those interpreted as (unrealistically) too old, we used OxCal 4.4 (Bronk Ramsey et al. 2021) to model the age of the north to south retreat of the MnIS. After recalibrating our new ages in addition to the existing ages of Bradwell et al. (2021), Small et al. (2012), Best et al. (2022) and Simms et al. (2022) using an OxCal Bayesian sequencing model, we find that the former MnIS started its retreat from the Gairloch area, to the north of the study site, 20.7 ± 1.2 ka and reached Strollamus, to the south of the study site, by 16.0 ± 0.2 ka. If we remove this age and instead use the modeled ages of 15.4 ± 1.0 ka and 14.3 ± 1.8 ka at Strollamus from Best et al. (2022) (sourced from Walker et al. (1988), Bradwell et al. (2019)) and Small et al. (2012), we find that on average the former MnIS retreated between ~16.2-19.5 ka (Fig. 7c). However, with our OSL errors between 1-5 ka in magnitude further refinement of this chronology may be warranted.

5.2.3 Wester Ross Readvance

Five of our OSL ages are located inside the boundary of the WRR based on the limits mapped by Robinson and Ballantyne (1979), Sissons and Dawson (1981), Ballantyne et al. (2009), Ballantyne and Stone (2012), Ballantyne and Bradwell (2021), Bradwell et al. (2021), and Bradwell and Stoker (2023) (Fig. 6). Recent studies have suggested the WRR occurred ~14-16.5 ka (Ballantyne and Stone, 2012; Bradwell et al. 2021; Simms et al. 2022). The five samples located inside the WRR include the raised beach plains at Firemore Beach (GA22-07), Second Coast (GA22-16), Badluarach (GA22-17), and Achiltibuie (UL22-04), as well as the delta at Loggie, near Ullapool (UL22-01).

Removing the Loggie sample (UL22-01), as discussed in sections 5.1.2, the remaining samples, from Firemore Beach (GA22-07), Second Coast (GA22-16), Badluarach (GA22-17), and Achiltibuie (UL22-04), exhibit ages of 18.5 ± 2.6 ka, 16.4 ± 2.2 ka, 18.3 ± 2.4 ka, and 14.6 ± 2.0 ka (Fig. 6). All four OSL samples returned ages within error of previous TCN ages reported by Bradwell et al. (2021), (15.2 ± 1.4 ka, 15.3 ± 2.2 ka, 15.2 ± 1.6 ka), as well as radiocarbon ages from Simms et al. (2022), (15.9 ± 0.2 ka, 15.9 ± 0.5 ka). By combining these ages in an OxCal probability distribution model (Fig. 7c), we estimate the end of the WRR to be approximately 15.8 ± 1.0 ka, consistent with previous estimates.

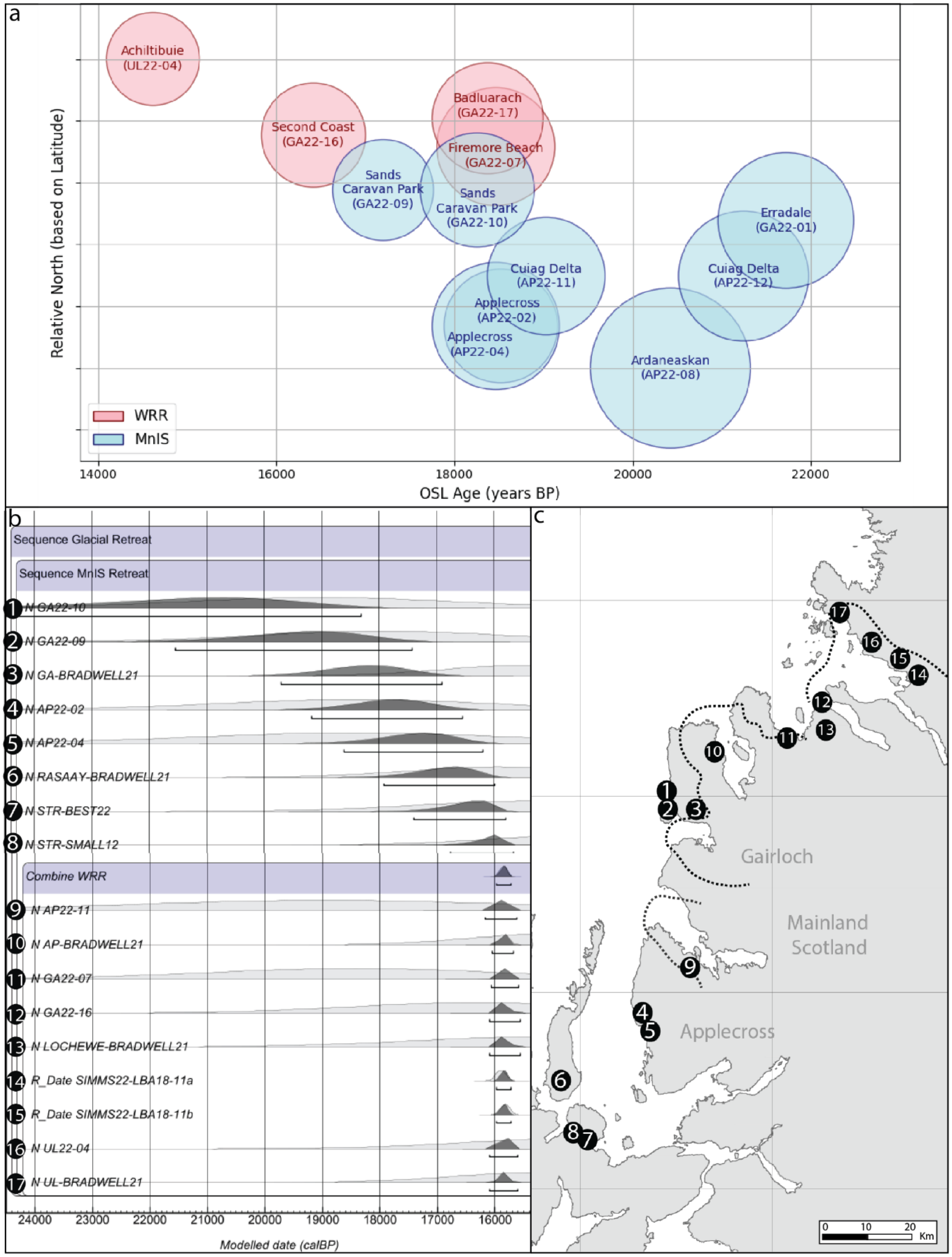

Figure 7. OSL ages of the Lateglacial shoreline. (a) Plot of OSL ages and errors presented in this study both outside (in blue) and inside (in red) the WRR boundary with their relative location to each other

based on latitude. The x-axis contains the OSL age of each sample while the size of each circle is directly proportional to the error. This graph reveals no significant relationship between OSL age and location progressing northward. (b) OxCal Bayesian sequence model with probability distributions of OSL ages for the MnIS and the WRR (Bronk Ramsey et al. 2021) with additional ages from Bradwell et al. (2021), Small et al. (2012), Best et al. (2022) and Simms et al. (2022). X-axis is modeled age (calBP). (c) Locations of ages for OxCal sequence modeling.

5.3 Implications for RSL: Comparison with GIA Prediction

We compared our RSL observations with predictions from three GIA models for NW Scotland: PaleoMIST (Gowan et al. 2021), GLAC1D (Tarasov et al. 2012), and Bradley-Hybrid (Bradley et al. 2023) (Fig. 8). These models all adopt a noncircular approach, using independent evidence for paleo-ice sheet extent and thickness, empirically derived from data constraining the ice sheet itself rather than relying solely on ice sheet reconstructions to match sea-level data.

All three models predict a higher marine limit farther south near Strollamus, Applecross, and the Cuaig delta, as they are more near the center of uplift, compared to sites more northward near Second Coast, Badluarach, and Achiltibuie. Although the marine limit observations for Applecross and the Cuaig Delta from this study are not within error of the GIA model predictions, they maintain this same general trend as the model predictions: a decreasing marine limit moving south to north (Fig. 5).

Although the GIA models produce similar RSL predictions, the Bradley-Hybrid and GLAC1D models, which are based on the same ice sheet reconstructions (British-Irish and Eurasian Ice Sheets), suggest an earlier RSL fall due to older ice-free conditions (16 ka) compared to the PaleoMIST model (15 ka). In contrast, the PaleoMIST model—developed independently of indirect proxy data and far-field sea-level records—predicts consistently higher marine limits across all sites and a higher RSL up until the Holocene. This discrepancy likely reflects the use of a thicker ice-sheet reconstruction in the PaleoMIST model. The younger deglaciation of the PaleoMIST model leads to a later RSL fall, resulting in less agreement with our new OSL ages compared to the Bradley-Hybrid and GLAC1D models (Fig. 8).

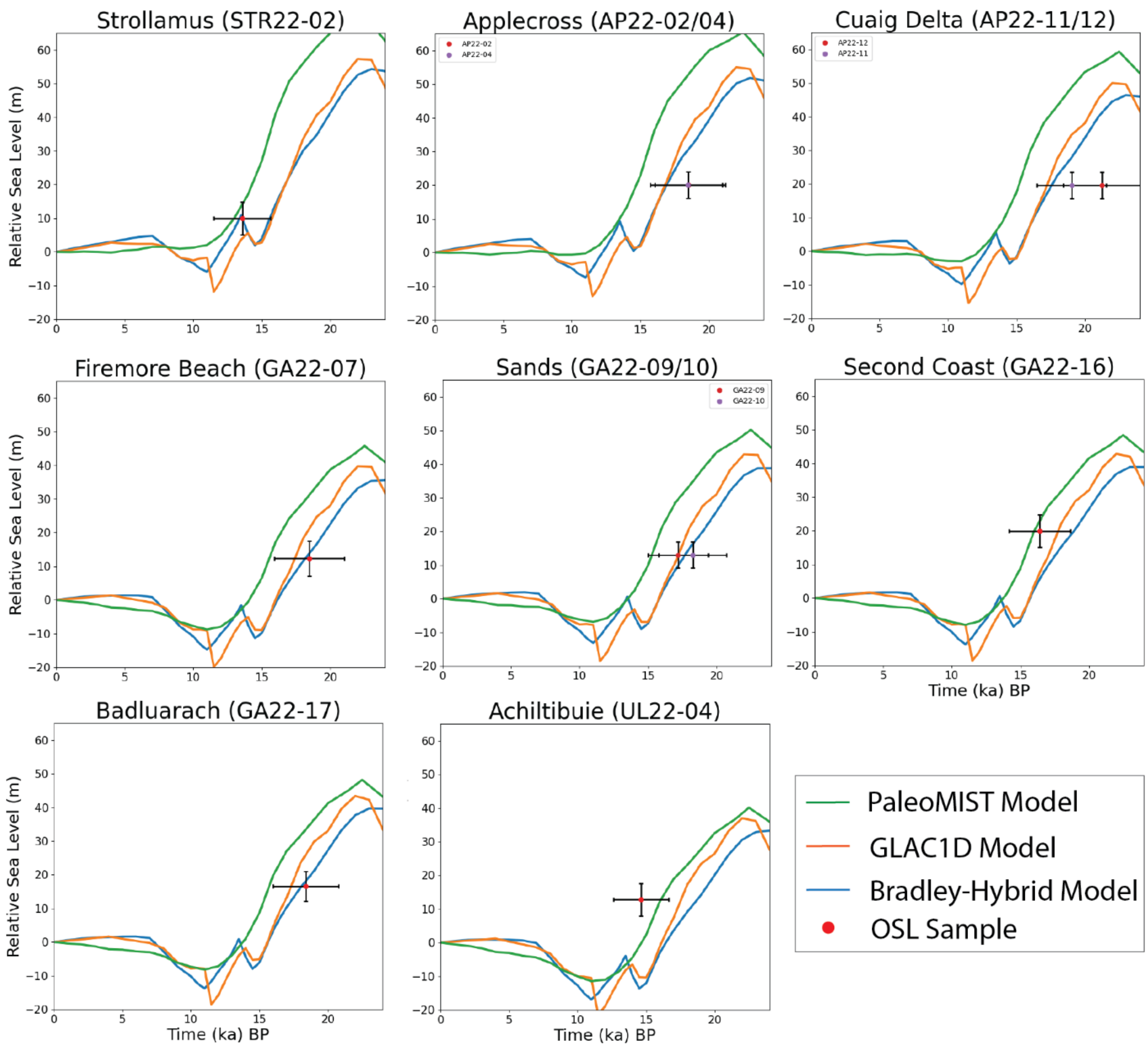

Figure 8. Comparison of predicted GIA RSL histories from three separate models with observed RSLs from this study. Predictions are based on the following GIA models: PaleoMIST (green), GLAC1D (orange), Bradley-Hybrid (blue), while observed RSLs are indicated by a red marker with their relative 2 sigma errors.

6. Conclusions

We provide new OSL ages on the Lateglacial shorelines along the flanks of the former MnIS of NW Scotland to provide better constraints on RSL during the last deglaciation. Although many of our OSL ages are older than expected, in general our new ages confirm the Lateglacial age of these shorelines, directly dating these features for the first time. Disregarding the anomalously old ages and including previously published ages of the WRR moraines, four ages located within the limits of the WRR, ranging between 14.6 ± 2.0 ka and 18.5 ± 2.6 ka suggest an age of 15.8 ± 1.0 ka for the WRR. The remaining deglacial OSL ages, situated outside of the WRR ice-sheet moraines, range in age from 13.6 ± 2.0 ka to 18.5 ± 2.8 ka. These new OSL ages refine the timing of rapid retreat of the former MnIS from 15.5-18.5 ka to between ~16.2-19.5 ka. Comparison of our results with three GIA-model RSL predictions show general agreement, but favor ice models with an earlier deglaciation. While our new ages suggest ice-sheet retreat in mainland NW Scotland may have occurred earlier than previously suggested, large uncertainties associated with the technique highlight the need for more age constraints.

Acknowledgements

We would like to thank Jennifer Taylor, Elisa Medri, Claire Divola, and Chris Garcia for their help in the lab and field, as well as the landowners in NW Scotland for granting access to their land.

EH, ARS and RDW funded by US National Science Foundation grant number EAR-2147750. LB, TB, JML and SLB funded by UK Natural Environment Research Council (NERC) grant numbers NE/X009343/1, NE/X009378/1, NE/X009335/1 and NE/X009459/1, respectively.

Supplementary Material

The following are Optically Stimulated Luminescence (OSL) dated samples from raised beaches, fluvial terraces, and deltas containing site images as well as sedimentary stratigraphic columns.

Fig S1. Sedimentary stratigraphic columns
Fig S2. OxCal probability output
Table S1. Summary of OSL ages not included in the results section of the text.

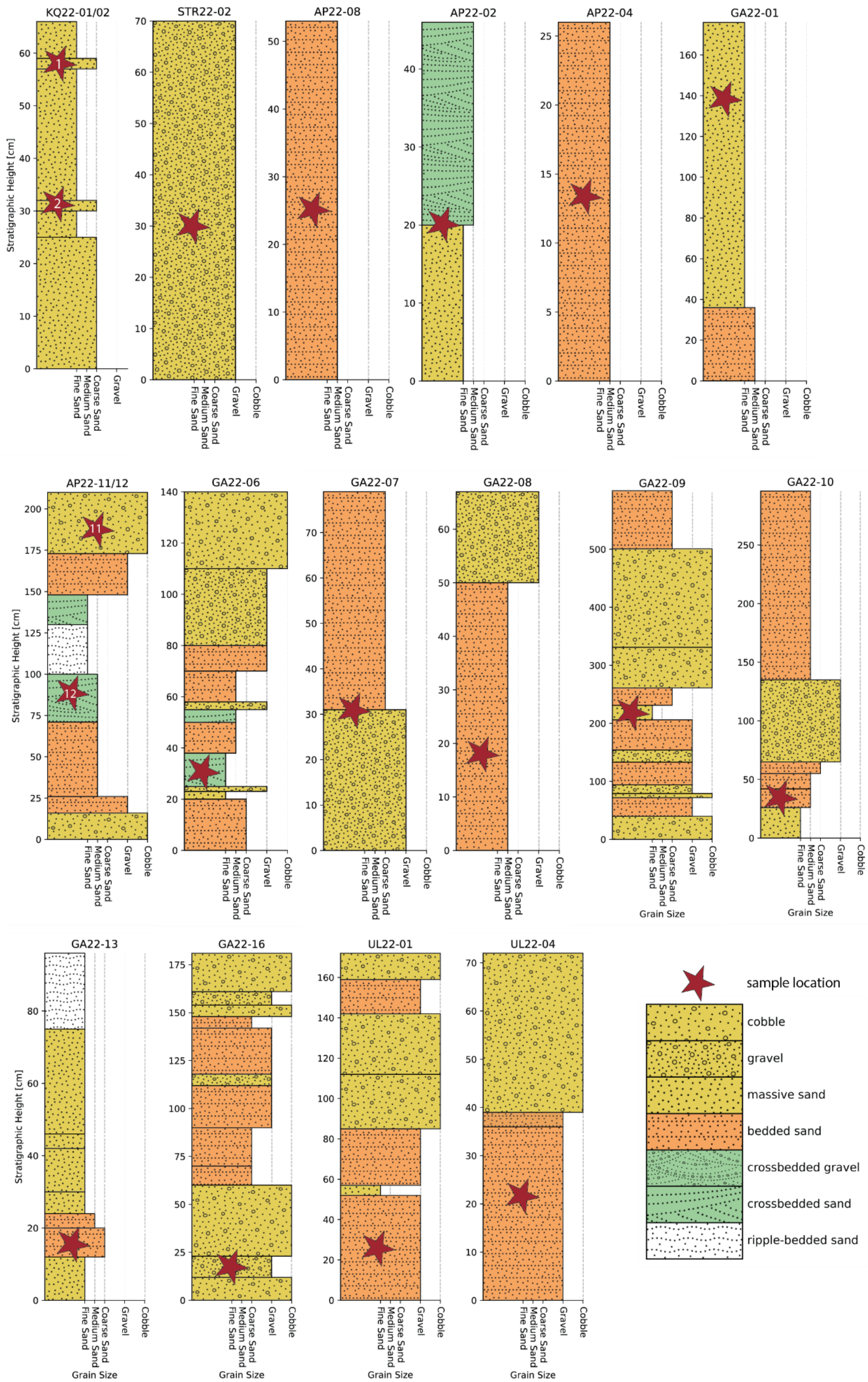
KQ22-01/02
STR22-02
AP22-08
AP22-02
AP22-04
GA22-01
AP22-11/12
GA22-06
GA22-07
GA22-08
GA22-09
GA22-10
GA22-13
GA22-16
UL22-01
UL22-04
Stratigraphic Height [cm]
Fine Sand
Medium Sand
Coarse Sand
Gravel
Cobble
Grain Size
sample location
cobble
gravel
massive sand
bedded sand
crossbedded gravel
crossbedded sand
ripple-bedded sand

Fig S1. Sedimentary stratigraphic columns for all samples targeted for dating in this study with specified grain size, sedimentary structures, and section type.

Name	Unmodelled (BP)		Modelled (BP)		Indices A_{model}=117.7 $A_{overall}$=112					Controls		
	from_95.4	to_95.4	from_95.4	to_95.4	A_{comb}	A	L	P	C	Select	Page	Edit
▼ Sequence Glacial Retreat										2		
▼ Sequence MnIS Retreat										3		
N GA22-10	23829	14229	24501	18309		90.9			99.9	4		
N GA22-09	22329	13529	21537	17423		108.1			100	5		
N GA-BRADWELL21	18330	12730	19702	16902		27.6			99.9	6		
			Warning! Poor agreement - A= 27.6%(A'c= 60.0%)									
N AP22-02	23229	13629	19170	16554		132.3			100	7		
N AP22-04	24029	12829	18610	16202		129			100	8		
N RASAAY-BRADWELL21	19139	12739	17914	15994		115.4			100	9		
N STR-BEST22	19329	11329	17390	15790		118.1			100	10		
N STR-SMALL12	17839	10639	16764	15666		81.3			100	11		
▼ Phase Ice Readvance										12		
▼ Combine WRR	15980	15739	15969	15728	146.1				98.5	13		
N AP22-11	25729	12129	16162	15618		93.7			100	14		
N AP-BRADWELL21	17930	12330	16048	15684		124			100	15		
N GA22-07	23629	13229	16064	15596		86.3			100	16		
N GA22-16	20729	11929	16088	15560		138			100	17		
N LOCHEWE-BRADWELL21	19630	10830	16088	15560		135.9			100	18		
R_Date SIMMS22-LBA18-11a	16071	15722	15969	15728		102.9			98.5	19		
R_Date SIMMS22-LBA18-11b	15988	15669	15969	15728		110.3			98.5	20		
N UL22-04	18529	10529	16090	15610		113.8			100	21		
N UL-BRADWELL21	18330	11930	16090	15610		127.9			100	22		

Fig S2. OxCal probability output for a Bayesian sequence probability function

Sample	Mineral	Crystal size (µm)	Aliquot	Equivalent Dose (Gy)	Dose error (Gy)	OD (%)	Dose rate (Gy/ka)	Dose rate error (Gy/ka)	Age (ka)	Age error (ka)
KQ22-01	K-fsp	90-150	28	275	15.1	7.5	2.724	0.140	111491	8338
KQ22-05	K-fsp	90-150	28	337	18.9	7.4	2.995	0.140	178494	13558
TB22-01	quartz	90-125	20	184	14.3	18	2.389	0.175	76898	8220
TB22-02	quartz	90-125	22	172	12.5	16	1.845	0.085	93096.2	8014
TB22-03	quartz	90-125	26	139	11.0	22	2.950	0.121	47113	4210
AP22-14	quartz	150-180	29	305	23.1	26	2.901	0.097	105075	8723
UL22-03	Na-fsp	125-50	27	101	5.50	6.3	2.996	0.100	42686	2431

Table S1. Summary of OSL ages mentioned in the discussion, but disregarded from the results section. Ages for K-feldspars represent fading-corrected ages.